BOLETÍN DE LA SOCIEDAD ESPAÑOLA DE CERÁMICA Y VIDRIO XXX (2021) XXX–XXX

BOLETIN DE LA SOCIEDAD ESPAÑOLA DE
Cerámica y Vidrio
www.elsevier.es/bsecv

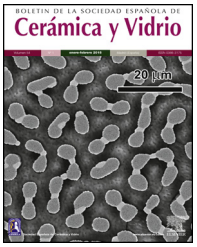

Original

Alkali-activated binders based on the coarse fraction of municipal solid waste incineration bottom ash

Alex Maldonado-Alameda, Jessica Giro-Paloma, Jofre Mañosa, Joan Formosa, Josep Maria Chimenos *

Departament de Ciència de Materials i Química Física, Universitat de Barcelona, Barcelona, Spain

ARTICLE INFO

Article history:
Received 17 July 2020
Accepted 22 December 2020
Available online xxx

Keywords:
Bottom ash
MSWI
Waste management
Low-carbon cements
Alkali-activated binder

ABSTRACT

The potential of the least polluted fraction (from 8 to 30 mm) of municipal solid waste incineration (MSWI) weathered bottom ash (WBA) as an alkali-activated cement precursor was evaluated. Alkali-activated WBA binders (AA-WBA) formulations were prepared through alkali-activation of WBA as sole precursor. Sodium silicate (Na_2SiO_3) and sodium hydroxide (NaOH) mixtures with different pH's were used as alkali-activator solution. The effect of alkali-activator solution pH on the final properties was assessed. Results showed the hydrolytic stability of all formulations. The selective chemical extractions and physicochemical characterisation revealed the formation of the C–S–H, C–A–S–H, and (N,C)–A–S–H gels. The promising compressive strength results demonstrated the potential of AA-WBA binders. The increase of pH in the alkali-activated solution promotes the formation of gel reaction products and enhance mechanical properties. This investigation promotes the green cements manufacturing and the use of secondary resources to reduce the impact of natural resources extraction used for the ordinary Portland cement (OPC) production.

Aglutinantes alcalinos basados en la fracción gruesa de las escorias de incineración de los residuos urbanos

Palabras clave:
Escoria
Escorias de incineracion
Gestión de residuos
Cementos de bajas emisiones
Aglutinantes alcalinos

RESUMEN

En el presente trabajo se evaluó el potencial como material precursor de la escoria procedente de la incineración de residuos urbanos (MSWI BA) en la formulación de cementos alcalinos. La fracción menos contaminada de escoria (8-30 mm), previamente madurada, se usó como único precursor para la formulación de aglutinantes alcalinos (AA-WBA). Como solución activadora se emplearon varias mezclas de silicato sódico (Na_2SiO_3) e hidróxido de sodio (NaOH) con diferentes concentraciones para evaluar el efecto del pH del activador en

* *Corresponding author.*
E-mail address: chimenos@ub.edu (J.M. Chimenos).
https://doi.org/10.1016/j.bsecv.2020.12.002

Please cite this article in press as: A. Maldonado-Alameda, et al., Alkali-activated binders based on the coarse fraction of municipal solid waste incineration bottom ash, Bol. Soc. Esp. Cerám. Vidr. (2021), https://doi.org/10.1016/j.bsecv.2020.12.002

las propiedades finales del material. Los resultados verificaron la estabilidad hidrolítica de todas las formulaciones. La selección química extractiva y la caracterización físico-química reveló la formación de geles C-S-H, C-A-S-H y (N,C)-A-S-H. Los prometedores resultados de resistencia a compresión demostraron el potencial de los AA-WBA. El incremento del pH de la solución activadora contribuye a la formación de los productos de reacción y mejora las propiedades mecánicas. Esta investigación promueve la fabricación de cementos más respetuosos con el medio ambiente y el uso de materias primas provenientes de fuentes secundarias para minimizar la extracción de recursos naturales utilizados en la fabricación de cemento Portland.

Introduction

Ordinary Portland cement (OPC) is the most used building material due to its mechanical properties, abundance, and low cost. The OPC manufacturing is energy-intensive since requires combustion processes at high temperatures (1450 °C) as well as heavy equipment to crush and grind the raw materials and clinker [1]. In 2019, the worldwide OPC production was 4.1 billion tonnes [2]. Emerging economies (e.g. China and India) were responsible for 60% of the global OPC production because of their economy and population growth. For these reasons, the OPC manufacturing is responsible for 5–7% of global anthropogenic CO_2 emissions [3] and the 2% of the global primary energy consumption [4]. Excessive OPC production has become an important threat to the population health and the environment [5,6]. The main challenge for the cement industry is seeking more efficient manufacturing processes and new eco-friendly materials, promoting the new low-carbon strategies and policies raised by the governments [7]. Focusing on the investigation and the development of new sustainable materials, one of the leading and promising alternatives are the alkali-activated cements (AACs) [8].

AACs are a high strength binder system consisting of the reaction of an alkali-activating solution with a solid aluminosilicate-rich powder precursor [9]. The alkali media, usually sodium hydroxide (NaOH), potassium hydroxide (KOH), and sodium silicate (Na_2SiO_3) [10], accelerates the dissolution of the solid precursor. After a proper curing process, a binder matrix with similar properties to the OPC is obtained [11]. The main reaction products are C–A–S–H, N–A–S–H, or (N,C)–A–S–H gels depending on the calcium availability in the powder precursor [12]. Binder's final microstructure and properties also vary as a function of the alkali activator used [13], and the curing temperature [14,15]. The mechanical properties and high resistance to temperature and fire are the most highlighted AACs properties [16,17]. However, their highest added value is their low carbon footprint compared to OPC [18]. The energy reduction required for their production turns AACs into a greener material than OPC [8]. The use of municipal and industrial wastes [19,20] as prevalent precursors is also remarkable because it allows moving towards zero waste principle promoted by the European Union (EU) [21].

The bottom ash (BA) from municipal solid waste incineration (MSWI) is a potential precursor in AACs, as demonstrated in some recent publications [22–24]. In 2018, 250 million tonnes of MSW were generated in the 28 countries of the EU (EU-28). The leading European states base a large part of their waste management policy on energy recovery through incineration [25]. Around 28% of MSW in the EU-28 (2018) were incinerated in waste-to-energy plants (WtE) [26]. The incinerated bottom ash (IBA) production in 2017 was 19 Mt, which is approximately 20 wt.% of the waste treated in the plants in the EU-28 [27,28]. IBA is mainly composed of mineral fraction (85%), ferrous metals (10–12%), and non-ferrous metals (2–5%) [27]. The mineral fraction can be considered a slag and granular material and it is classified as hazardous or non-hazardous waste according European waste codes (EWC). For its application in a wide range of engineering sectors [29], it is necessary a weathering process for 2–3 months to carbonation, pH stabilisation, and hydration of the IBA mineral phases [30]. Weathered bottom ash (WBA) is the technical name of the resulting material after this maturation process. Despite the high WBA heterogeneity, its composition is silica-rich and contains substantial amounts of calcium and aluminium [31,32]. These are the essential compounds to obtain AACs. Therefore, it is demonstrated that WBA can be considered as a potential source in the AACs formulation [24]. Although the WBA potential in the AACs formulations has been demonstrated elsewhere [24], just a few studies use WBA as sole precursor. The AACs formulated with WBA stand out for their high porosity [33] which is directly related to the metallic aluminium content in the powder precursor. During the AACs reaction process, the alkali media reacts with the metallic aluminium generating hydrogen gas [34]. Therefore, AACs for non-structural purposes are obtained [23,35], due to its high porosity and low compressive strength values.

The aim of this study is the use of the least polluted fraction of the WBA (from 8 to 30 mm) as sole precursor to formulate new sustainable alkali-activated binders (AA-WBA). Although WBA is extensively used as secondary aggregate in civil engineering, its valorisation as precursor is a great opportunity to give it an added value and promote the zero-waste cement manufacturing. In addition, the WBA alkali-activation promotes the use of secondary resources instead the natural resources exploitation associated to the clinker production. The novelty of this study is the use of the 8–30 mm fraction instead of 0–30 mm fraction [35] to enhance the mechanical properties of final AA-WBA. The 8–30 fraction is mainly composed by container glass and fired ceramics, and it was chosen considering previous studies carried out by the authors, where the highest SiO_2 availability was demonstrated to be in the

Please cite this article in press as: A. Maldonado-Alameda, et al., Alkali-activated binders based on the coarse fraction of municipal solid waste incineration bottom ash, Bol. Soc. Esp. Cerám. Vidr. (2021), https://doi.org/10.1016/j.bsecv.2020.12.002

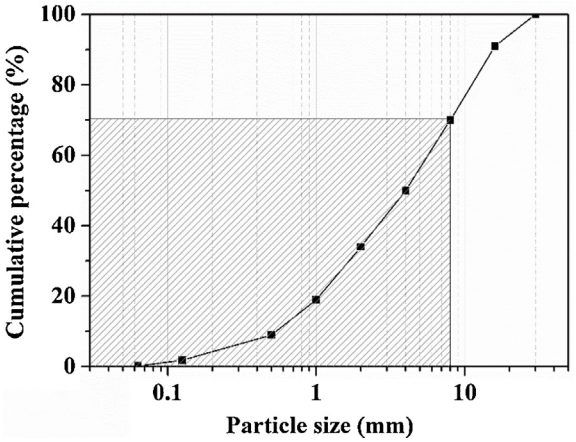

Fig. 1 – Particle size distribution (PSD) of WBA.

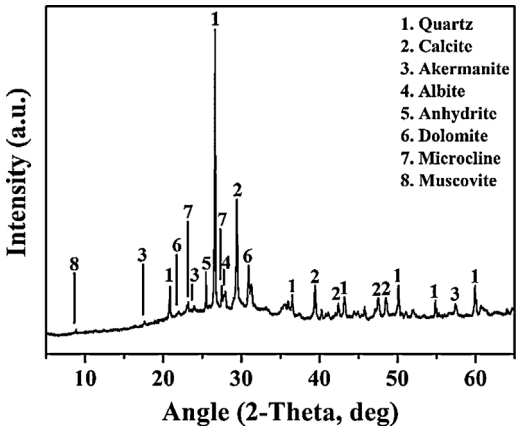

Fig. 2 – XRD pattern of WBA.

fractions above 8 mm [24]. It is expected that higher SiO_2 availability on WBA (from 8 to 30 mm) enhance the precursor reactivity during the alkali activation process and the binders' compressive strength. Moreover, the least polluted fraction contains less amount of metallic aluminium and therefore the generation of hydrogen gas will be lower than other studies carried out by the authors [35]. The curing process was performed at room temperature to favour the manufacture as well as to expand the applicability of the AA-WBA. The AA-WBA binders were formulated using sodium silicate (Na_2SiO_3) and NaOH solutions at different concentrations. The NaOH concentration effect on the final AA-WBA properties was studied from physicochemical, mechanical, and environmental point of view.

Experimental details

Materials

The WBA was collected from a WtE plant located in Tarragona (Spain), which incinerates around 380 t day^{-1} of MSW. After recovering ferrous and non-ferrous metals in a treatment process, and removing lightweight unburned materials, around 88 t day^{-1} of fresh IBA are obtained. Finally, the obtention of WBA is produced when the fresh IBA is stockpiled outdoors for 2–3 months to stabilise the heavy metal(loid)s. The collected WBA (25 kg) was dried in an oven at 105 °C for 24 h and subsequently sieved to obtain the 8–30 mm fraction. This fraction represents approximately the 30% of the total sample, as it is shown in particle size distribution in Fig. 1 (shaded zone was discarded). This 30% is mainly composed by ceramic materials, as well as primary and secondary glass [32]. After sieving, the WBA was crushed and milled until the whole fraction presented a particle size below 80 μm. The crystalline phases of WBA powder were determined by means of a Bragg–Brentano Siemens D-500 powder diffractometer equipment with Cu Kα radiation. The X-ray diffraction (XRD) pattern of the WBA (Fig. 2) confirms the presence of quartz (SiO_2; PDF# 01-079-1910) and calcite ($CaCO_3$; PDF# 01-083-1762) as main crystalline phases. Dolomite ($CaMg(CO_3)_2$; PDF# 01-075-1759), akermanite ($Ca_2Mg(Si_2O_7)$; PDF# 01-079-2424), anhydrite ($CaSO_4$; PDF# 01-072-0503), albite calcian ordered ($(Na,Ca)Al(Si,Al)_3O_8$); PDF# 020-0548), microcline ($KAlSi_3O_8$; PDF# 01-076-0918), and muscovite ($KAl_2(AlSi_3O_{10})(OH)_2$; PDF# 01-077-2255) were also detected. The XRD results agree with previous studies where was demonstrated that coarser fractions of the WBA contain a large amount of natural and synthetic ceramics, as well as substantial amounts of primary and secondary glass [32]. The chemical composition of the WBA powder was conducted by X-ray fluorescence (XRF) analysis with a spectrophotometer Panalytical Philips PW 2400 sequential X-ray equipped with the software UniQuant® V5.0. Table 1 shows major and trace elements, and confirms that the main compounds are SiO_2, CaO, and Al_2O_3. This fraction presents a substantial lack of aluminium due to the high amount of non-ferrous metals recovered by Eddy current device in the fractions above 6 mm [27]. The presence of Al_2O_3 comes from fired ceramics as mentioned above. XRF results also agree with the XRD results and the previous studies mentioned above. The alkali-activator solution used is composed of Na_2SiO_3 and NaOH mixture. The Na_2SiO_3 solution with 26.44% of SiO_2 and 8.21% of Na_2O ($\rho = 1.37$ g cm^{-3}) was provided by Scharlab, S.L. company. NaOH solutions (2M ($\rho = 1.08$ g cm^{-3}); 4M ($\rho = 1.16$ g cm^{-3}); 6M ($\rho = 1.20$ g cm^{-3}); and 8M ($\rho = 1.24$ g cm^{-3})) were prepared by dissolving NaOH pearls (Labbox Labware S.L.; purity >98%) in deionised water.

AA-WBA preparation

The alkali-activator (Na_2SiO_3/NaOH) to precursor (WBA) ratio remains constant in all the formulations and only the concentration of the NaOH solution was varied. Table 2 shows the mix proportion and chemical composition of alkali-activator solution. The liquid-to-solid (L/S) mass ratio was determined considering the good workability of the fresh AA-WBA pastes during mixing and casting processes. This parameter was determined by means mini-slump test procedure reported in the literature [36]. The spread diameters were comprised in a range between 120 and 140 mm. Liquid (L) term is referred to the mixture of Na_2SiO_3 and NaOH solutions. Solid (S) term is attributed exclusively to the WBA powder. The preparation of AA-WBA was initiated mixing NaOH and Na_2SiO_3 solutions (mass ratio of 1:4) in a plastic beaker. This proportion

Please cite this article in press as: A. Maldonado-Alameda, et al., Alkali-activated binders based on the coarse fraction of municipal solid waste incineration bottom ash, Bol. Soc. Esp. Cerám. Vidr. (2021), https://doi.org/10.1016/j.bsecv.2020.12.002

Table 1 – Major, minor, and trace elements composition of WBA powder.

Major elements (wt.%)										
SiO_2	CaO	Al_2O_3	Na_2O	K_2O	Fe_2O_3	MgO	TiO_2	Cl^-	SO_3	LOI
52.08	20.72	6.35	3.38	2.09	4.12	2.43	0.65	0.54	1.07	6.10

Minor and trace elements (wt.%)												
Mn	Cu	Zn	Br	Rb	Sr	Y	Zr	Nb	Sn	Sb	Ba	Pb
0.02	0.04	0.12	<0.01	0.01	0.05	<0.01	0.10	<0.01	0.01	0.01	0.04	0.04

Loss on ignition at 1100 °C.

Table 2 – Mix proportion and alkali-activator chemical composition.

Reference	S	L					[a]Na_2O (wt.%)	[b]SiO_2/Na_2O	pH
	WBA	[a]NaOH (wt.%)				[a]Na_2SiO_3 (wt.%)			
		2M	4M	6M	8M				
AA-WBA-2M	100	16				64	6.2	2.83	11.43
AA-WBA-4M	100		16			64	6.9	2.51	11.90
AA-WBA-6M	100			16		64	7.7	2.26	12.18
AA-WBA-8M	100				16	64	8.4	2.06	12.68

[a] Respect to the WBA content.
[b] Molar ratio.

of alkali-activator solution responds to the main goal of this work, which is to enhance the mechanical properties of AABs formulated with WBA as the sole precursor. A NaOH higher proportion leads to a higher generation of hydrogen affecting to the mechanical properties of final samples [34]. The WBA and the alkali-activator solution were mechanically mixed (liquid-to-solid mass ratio of 0.8:1). The mixing procedure consisted of adding gradually the solid into the liquid for 2 min at 472 rpm to favour the dissolution of reactive phases. Afterwards, the whole mixture was mixed for 3 min at 760 rpm. The fresh pastes of AA-WBA were cast into 25 mm cubic moulds and sealed in plastic bags for 3 days in a climate chamber at 25 ± 1 °C and relative humidity of 95 ± 5%. After 3 days, the specimens were demoulded and kept in the climate chamber under the same conditions for 28 days. Nine cubic shape specimens were obtained from the same batch for each formulation. Four of these specimens were used for the compressive strength test. The fractured particles after the compressive strength test were ground to carry out the leaching test. These fractured particles were also milled to determine the physicochemical characterisation (excepting SEM characterisation) and selective chemical extraction. Finally, three more specimens were used to determine the apparent density and open porosity and two specimens for the boiling water test and SEM characterisation, respectively.

Experimental tests

Boiling water test

The hydrolytic stability and degradation of the AA-WBA samples were assessed through the immersion of the specimens (previously dried in a desiccator with silica gel until constant weight) in boiling water for 20 min [37]. Afterwards, the specimens were placed in a desiccator with silica gel until constant weight. Finally, the specimen was weighed before and after the test to determine the mass loss percentage and to certify the hydrolytic stability of all samples.

Selective chemical extractions

The selective chemical extraction is a complementary tool to the characterisation techniques which allows determining the gels nature formed during the AACs geopolimerisation process [38]. The main reaction products formed in calcium-rich precursors, such as WBA, are C–S–H or C–A–S–H gels [39]. These gels can coexist with sodium aluminosilicates or N–A–S–H gels obtaining a binder matrix with (N,C)–A–S–H gel [38].

The salicylic acid/methanol (SAM) extraction was conducted to dissolve calcium silicate hydrate phases (C–S–H and C–A–S–H gels) of the AA-WBA formulated [38]. The SAM process consisted of adding 1 g of milled sample in a solution of salicylic acid (6 g) and methanol (40 ml) and stirring for 1 h [23]. Later the solution was filtered (cellulose filter with 20 μm pore size), and the insoluble residue was washed with methanol and placed in a desiccator until constant weight. Finally, the insoluble residue was weighed to determine the weight loss percentage.

The HCl extraction method was performed to dissolve both calcium silicate hydrate phases and the sodium aluminosilicate gels and zeolites [40]. For the HCl extraction, 1 g of powdered AA-WBA sample of each formulation was stirred in a plastic beaker containing a 250 ml HCl solution (1:20) for 3 h. Then, the solution was filtered (cellulose filter with 20 μm pore size), and the insoluble residue was washed with deionised water and dried in a desiccator until constant weight. The

Please cite this article in press as: A. Maldonado-Alameda, et al., Alkali-activated binders based on the coarse fraction of municipal solid waste incineration bottom ash, Bol. Soc. Esp. Cerám. Vidr. (2021), https://doi.org/10.1016/j.bsecv.2020.12.002

weight loss percentage was determined by weighing the insoluble residue.

Physicochemical characterisation

The main crystalline phases of AA-WBA samples were assessed with Bragg–Brentano Siemens D-500 powder diffractometer device with Cu Kα radiation. The formation of AA-WBA main reaction products and insoluble residues obtained in selective chemical extractions were also evaluated by Fourier transform infrared spectroscopy (FT-IR) in attenuated total reflectance mode (ATR). A Spectrum Two™ equipment from Perkin Elmer was configured for conducting measurements with an average of 32 scans in the range of 4000–400 cm^{-1} and a resolution of 4 cm^{-1}. The FT-IR spectra deconvolution of the AA-WBA binders were performed by means of computer software to acquire a complete understanding of the reaction products formed. The deconvolution was performed in the range of 1250–800 cm^{-1}, corresponding to the symmetric and asymmetric stretching vibrations of Si–O bonds [41]. Gaussian functions were added to adjust the shape of the spectra, following some criteria extracted from literature: (i) the presence of a shoulder or a slope variation in the FT-IR spectrum should correspond to the presence of a band; (ii) the addition of a peak improves the fit in the range and the coefficient of correlation; (iii) the coefficient of correlation should be always above 0.999 [42]. The fitting with the Gaussian functions was combined with the self-fitting function of the computer software. The microstructure characterisation of the samples was conducted through scanning electron microscopy (SEM), using an ESEM FEI Quanta 200 equipment. The CaO/SiO_2, Al_2O_3/SiO_2, and Al_2O_3/Na_2O ratios were determined through the energy-dispersive X-ray spectroscopy (EDS) analysis of the micrograph areas for each sample. The samples were cut with a diamond disc cutter at low velocity (140 rpm) to obtain a planar sample with 1.5 mm thickness for each formulation. The samples were coated with graphite due to the non-conductive nature of the AA-WBA binders. Bulk density and open porosity were determined following the EN 1936:2006 standard.

Mechanical characterisation

The compressive strength was evaluated by testing three specimens for each formulation. Specimens were evaluated through compressive strength test with an Incotecnic MULTI-R1 device, equipped with 20 kN load cell, following the standard UNE-EN 196-1. A progressive load until fracture (loading rate of 240 $kg\,s^{-1}$) was applied. The mean values for the four cubic shape specimens for each formulation were reported.

Leaching test

The environmental characterisation of the AA-WBA was performed following the European standard EN 12457-2 to assess the heavy metal(loid)s (As, Ba, Cd, Cr, Cu, Hg, Mo, Pb, Ni, Sb, and Zn) potential release in deionised water. Leaching tests were conducted to the crushed AA-WBA (below 4 mm) aiming to simulate when AA-WBA binders are demolished at the end of their life cycle as the worst possible scenario. The effect of the alkali-activator solution and the stabilising capacity of the AA-WBA was also evaluated. Aliquots of both WBA and AA-WBA leachates (3 replicas for each formulation) were analysed by means an ELAN 6000 inductively coupled plasma mass spectrometry (ICP-MS) from Perkin Elmer.

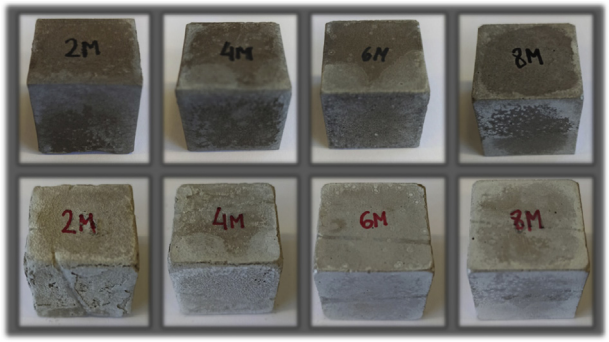

Fig. 3 – AA-WBA specimens before (up) and after (down) the boiling water test.

Table 3 – Selective chemical extraction results.

	Mass dissolved by SAM (wt.%)	Mass dissolved by HCl (wt.%)
OPC paste	89.8	–
WBA powder	5.5	27.1
AA-WBA-2M	18.8	36.6
AA-WBA-4M	21.1	38.6
AA-WBA-6M	23.6	39.2
AA-WBA-8M	24.7	40.8

Results and discussion

Boiling water test

The samples before and after the boiling test are shown in Fig. 3. All the samples succeed the test and there is no remarkable disaggregation, proving their hydrolytic stability and non-degradation. Some negligible disintegrations on the surfaces and the edges of the AA-WBA-2M and AA-WBA-4M samples can be observed. The appearance analysis agrees with the weight loss percentage results, which were 1.3% in AA-WBA-2M, 1.1% in AA-WBA-4M, and below 0.8% in AA-WBA-6M and AA-WBA-8M. Hence, the specimens presented the expected integrity, showing that these formulations resisted to hydrolytic degradation and maintained the structural consistency. This fact indicates that the specimens were properly bonded probably due to the alkali-activation of the precursor.

Selective chemical extraction

The dissolved percentage mass after selective chemical extraction test is summarised in Table 3. SAM extraction was also conducted to compare the differences between a common hydrated cement (OPC) with the alkali-activated binders formulated. The contrast is very remarkable since the OPC paste is mainly composed of calcium silicates hydrates (C–S–H) while the WBA composition is highly heterogeneous as seen in section "Materials". It is also observed a substantial increase

Please cite this article in press as: A. Maldonado-Alameda, et al., Alkali-activated binders based on the coarse fraction of municipal solid waste incineration bottom ash, Bol. Soc. Esp. Cerám. Vidr. (2021), https://doi.org/10.1016/j.bsecv.2020.12.002

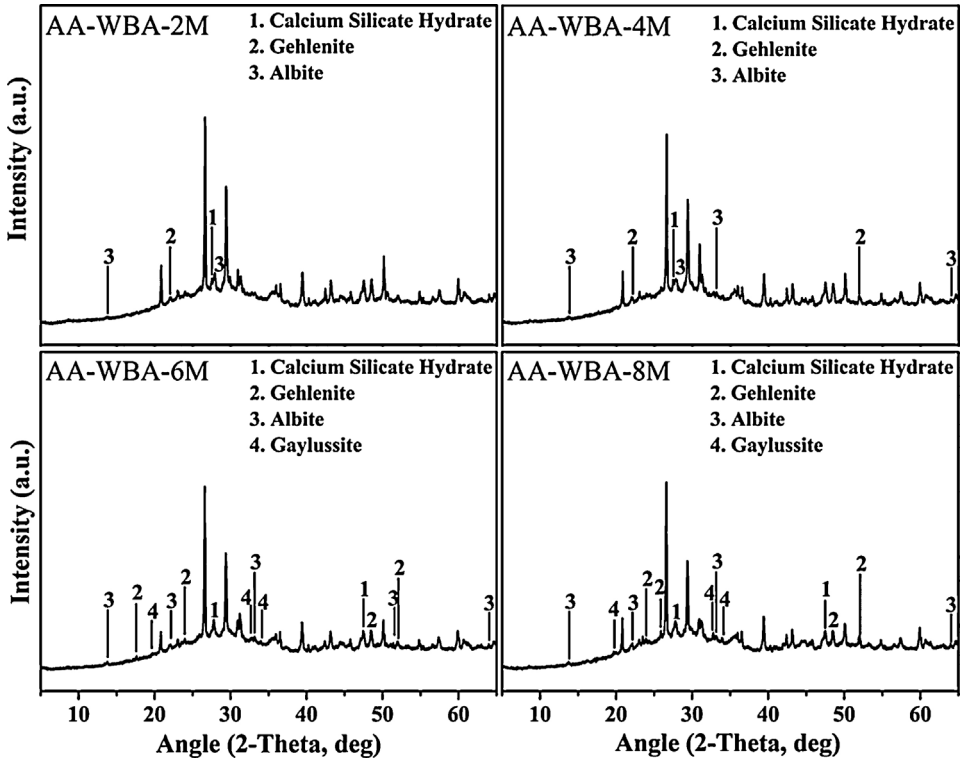

Fig. 4 – XRD patterns of AA-WBA samples.

in the mass dissolved between the WBA powder and AA-WBA samples. This fact revealed the formation of C–S–H and C–A–S–H gels [23,38] in all AA-WBA binders. It is remarkable that the mass dissolved by the HCl extraction was higher than SAM extraction since the former dissolved calcium (aluminium) silicate hydrate phases [43], sodium aluminosilicate gels [40], and carbonate phases [44]. The HCl extraction results demonstrated a probable formation of sodium aluminosilicate gels and dissolution of carbonates in all formulations.

Physicochemical characterisation

Fig. 4 depicts the new crystalline phases detected in the XRD patterns of the AA-WBA formulations. Calcium silicate hydrate (C–S–H; PDF# 01-072-1864), as well as gehlenite ($Ca_2Al(AlSi)O_7$; PDF# 025-0123), which is associated with the secondary products formed in the C–S–H gel [45], were detected in all formulations. A higher sodium rich phase of albite ($NaAlSi_3O_8$; PDF# 01-072-1245) was also identified in all pastes, which is attributed to N–A–S–H gel [46]. In the AA-WBA-6M and AA-WBA-8M formulations, gaylussite ($Na_2Ca(CO_3)_2{\cdot}5H_2O$; PDF# 020-1088) was also detected, which is a phase formed at early ages that indicates the cation exchange between the WBA and the alkali-activated solution [47]. The XRD results agree with those obtained in selective chemical extraction. The FT-IR spectra of the WBA and AA-WBA (Fig. 5) were assessed to verify the formation of the main reaction products (C–S–H, C–A–S–H, and N–A–S–H gels) compared to the initial WBA. It is observed a broad band (at 1200–900 cm^{-1}) in all cases, which is attributed to the stretching vibrations of Si–O [41]. The change in this band shape

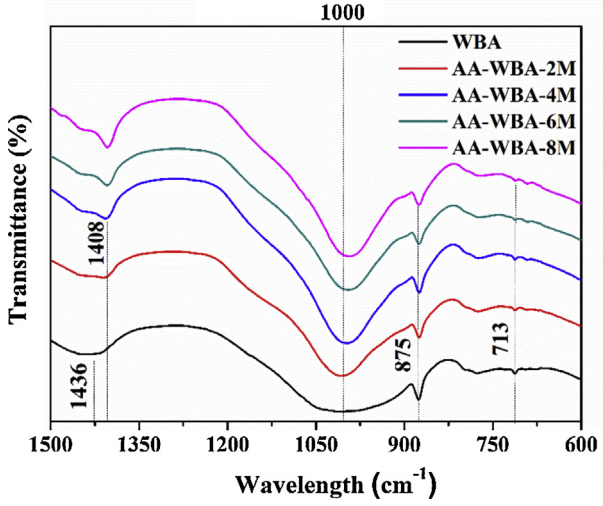

Fig. 5 – FT-IR spectra of AA-WBA samples.

and position revealed the formation of new phases due to the alkali-activation of WBA. The shift of the broad band at 1000 cm^{-1} (attributed to asymmetric T–O (T = Si or Al) stretching vibrations) demonstrates the alkali activation of the WBA [12]. It is appreciated that the increasing of the NaOH concentration displaces the band to lower frequencies [43]. This is probably due to both the inclusion of aluminium on the C–S–H gel [48] and the formation of N–A–S–H gels [40] in agreement with chemical extraction and XRD results. The band at 1408 cm^{-1} is ascribed to the formation of gaylussite ($Na_2Ca(CO_3)_2{\cdot}2H_2O$) [49]. The rest of the peaks were ascribed

Please cite this article in press as: A. Maldonado-Alameda, et al., Alkali-activated binders based on the coarse fraction of municipal solid waste incineration bottom ash, Bol. Soc. Esp. Cerám. Vidr. (2021), https://doi.org/10.1016/j.bsecv.2020.12.002

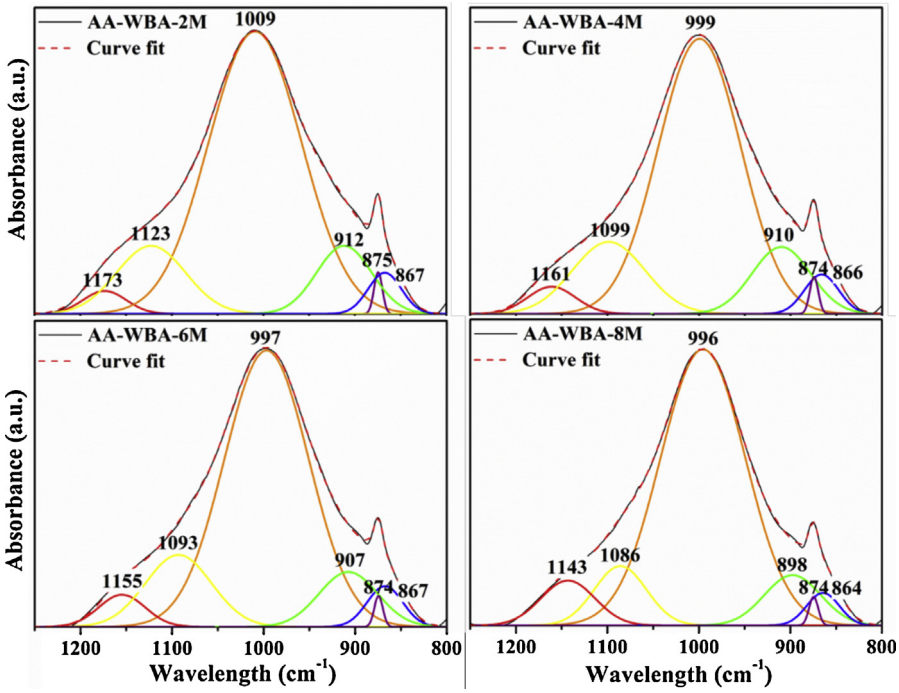

Fig. 6 – Deconvoluted spectra of AA-WBA samples in the range of 1250–800 cm^{-1}.

to the stretching (1436 cm^{-1}) and bending modes (875 cm^{-1} and 713 cm^{-1}) of carbonates [50].

In Fig. 6 are shown the deconvoluted spectra of the AA-WBA binders, which allow identifying and quantifying the different peaks and bands in the range of 1200–800 cm^{-1}. The main band at 1009–996 cm^{-1} is assigned to the ν_3(Si–O) stretching vibrations, typical in the activated pastes with waterglass [51]. This band shifts to lower wavenumber with a pH increase, as commented above [43]. In the four spectra, the bands at ~1090 cm^{-1} and ~1160 cm^{-1} are attributed to Q^3 and Q^4 silicon tetrahedra in a silica rich gel [43]. The band at ~905 cm^{-1} is assigned to the ν_2(Si–O) stretching vibrations. The narrow peak observed at ~875 cm^{-1} is associated to the presence of C–O stretching vibrations in carbonates [43]. The small band at ~865 cm^{-1} is ascribed to Si–O terminal vibrations, which may imply an incomplete polymerisation [52], as well as the presence of gaylussite. It should be emphasised the relevance of the peak at ~1000 cm^{-1} (see Fig. 6) which is associated to the formation of C–S-H and C–A–S–H gels [41].

Fig. 7 shows the FT-IR spectra of AA-WBA before and after the selective chemical extraction. The broad band around ~1000 cm^{-1} was displaced to a higher frequency in the residues of the extraction (1064 cm^{-1}) which demonstrated the dissolution of C–S–H and C–A–S–H phases by SAM and HCl extraction [38]. The three characteristic peaks of silica gel (790 cm^{-1}, 930 cm^{-1}, and 1050 cm^{-1}) were also observed after both selective extractions [53]. Finally, the peak attributed to gaylussite was dissolved in both extractions while the peak associated to bending modes of calcium carbonates remained after the HCl extraction [44].

The SEM micrographs in backscattering electron (BSE) mode of the AA-WBA are presented in Fig. 8. The AA-WBA binders' microstructure was similar except to AA-WBA-2M, which presented a less compact appearance. The lightest greyish compact area in all samples revealed the formation of C–S–H or C–A–S–H gels [51]. A darkest greyish colour matrix and a largest number of unreacted particles can be seen in the AA-WBA-2M sample. The rest of the formulations are similarly compacted although the AA-WBA-6M matrix seemed to be the most homogeneous and dense sample. Microcracks can also be appreciated in all pastes (except in the AA-WBA-2M sample) due to the drying shrinkage in this type of AACs [54].

The CaO/SiO_2, Al_2O_3/SiO_2, and Al_2O_3/Na_2O ratios of the lightest greyish compact areas of each sample were determined by EDS analysis (20 measures each). The results are summarised in Table 4. The CaO/SiO_2 ratios show the typical values for pastes formulated using waterglass as activator [16,51] while the Al_2O_3/SiO_2 and Al_2O_3/Na_2O ratios reveal a lack of aluminium content in all pastes. It is important to highlight that the higher the NaOH concentration, the higher the Al/Na ratio due to the aluminium inclusion into the C–S–H gels, as demonstrated in the displacement of the main band at ~1000 cm^{-1} (Figs. 5 and 6).

Physical and mechanical properties

The bulk density, open porosity, and compressive strength are key parameters to understand the behaviour of the AA-WBA formulated and to determine their potential applications. The bulk density (1.68 ± 0.1 g cm^{-3}) and open porosity (19.5 ± 0.5%) results were similar in all samples and their negligible difference did not justify the mechanical behaviour observed in Fig. 9.

A substantial increase in compressive strength was appreciated when the NaOH solution above 4 M in the alkali-activator solution was used. This fact was probably due to

Please cite this article in press as: A. Maldonado-Alameda, et al., Alkali-activated binders based on the coarse fraction of municipal solid waste incineration bottom ash, Bol. Soc. Esp. Cerám. Vidr. (2021), https://doi.org/10.1016/j.bsecv.2020.12.002

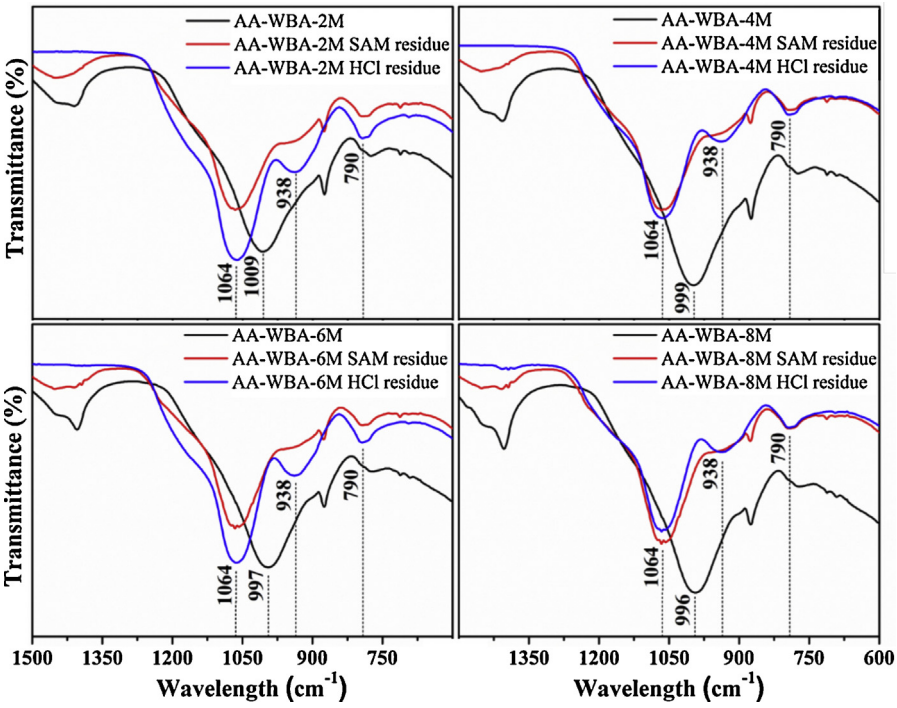

Fig. 7 – FT-IR spectra of AA-WBA samples before and after selective chemical extraction.

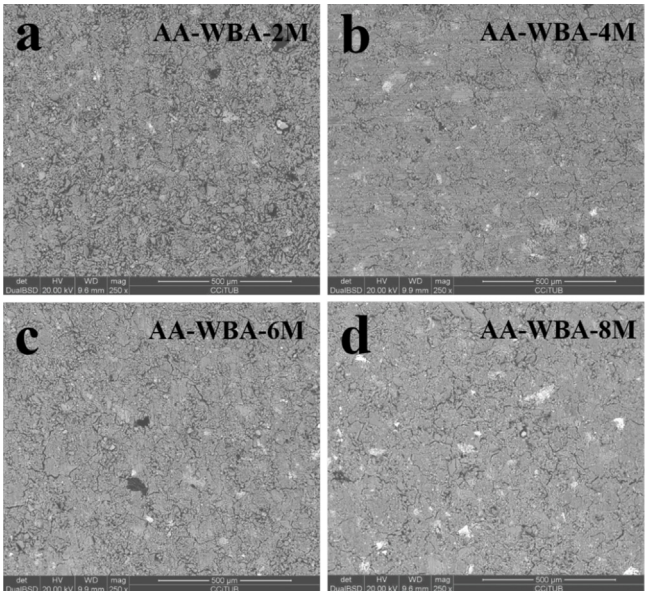

Fig. 8 – SEM micrographs of AA-WBA samples.

the increase in alkali dosage in alkali-activator solution (Na_2O wt.% by WBA weight), as well as to the decrease in silicate modulus (Ms; SiO_2/Na_2O ratio) as increase the NaOH concentration (Table 2). Other researchers revealed the influence of these two parameters in the mechanical properties of alkali-activated slags (AASs) [55]. The Ms and Na_2O% (by weight of slag) must be in the range of 0.75–1.25 and >6% to obtain good mechanical properties as reported elsewhere [56]. However, in the present study these Ms were not reduced more because it implied an increasing of NaOH proportion in the alkali-activator mixture. This increase in the NaOH proportion in the alkali-activator solution leads to a higher reactivity with metallic aluminium contained in the WBA generating hydrogen and reducing the mechanical properties [34]. The highest compressive strength value (22.8 MPa) was obtained in the AA-WBA-6M sample, which had a higher Ms (2.26) than AA-WBA-8M formulation (2.06). Therefore, the optimal modulus to obtain better compressive strength in the AA-WBA binders was found in the range of 2.0–2.5. It is important to highlight that the use of non-standard measures for the specimens influences the compressive strength results as reported elsewhere [57]. In the case of 25 mm cubic-shape specimens

Table 4 – SEM-EDS microanalysis of AA-WBA binders.

Reference	Weight percentage (wt.%)				Ratios by wt.%		
	Ca	Si	Al	Na	CaO/SiO_2	Al_2O_3/SiO_2	Na_2O/Al_2O_3
AA-WBA-2M	38.98	23.61	0.56	0.14	1.08	0.02	0.17
AA-WBA-4M	40.27	24.76	0.58	0.2	1.06	0.02	0.24
AA-WBA-6M	36.83	32.01	0.60	0.22	0.78	0.02	0.26
AA-WBA-8M	39.18	25.65	0.84	0.46	1.00	0.03	0.39

Please cite this article in press as: A. Maldonado-Alameda, et al., Alkali-activated binders based on the coarse fraction of municipal solid waste incineration bottom ash, Bol. Soc. Esp. Cerám. Vidr. (2021), https://doi.org/10.1016/j.bsecv.2020.12.002

Table 5 – Leaching concentrations (mg kg^{-1}) on WBA and AA-WBA binders after leaching tests (EN 12457-2) and limits for acceptance at landfills.

Sample	As	Ba	Cd	Cr	Cu	Hg	Mo	Pb	Ni	Sb	Zn	pH
WBA	0.02	0.25	<0.01	0.17	0.69	0.01	0.33	0.01	0.11	0.27	0.12	9.54
AA-WBA-2M	1.92	0.23	<0.01	1.00	1.130	0.029	0.460	0.80	0.18	1.42	1.03	11.32
AA-WBA-4M	2.21	0.23	<0.01	0.89	0.935	0.022	0.433	0.74	0.16	1.57	0.88	11.36
AA-WBA-6M	2.42	0.27	<0.01	0.57	0.972	0.024	0.409	0.65	0.17	1.59	0.65	11.36
AA-WBA-8M	2.47	0.18	<0.01	0.36	0.779	0.010	0.412	0.54	0.18	1.61	0.79	11.53
[a]Inert waste (mg kg^{-1})	0.5	20	0.04	0.5	2	0.01	0.5	0.5	0.4	0.06	4	
[a]Non-hazardous waste (mg kg^{-1})	2	100	1	10	50	0.2	10	10	10	0.7	50	
[a]Hazardous waste (mg kg^{-1})	25	300	5	70	100	2	30	50	40	5	200	

[a] Limit for acceptance at landfills [60].

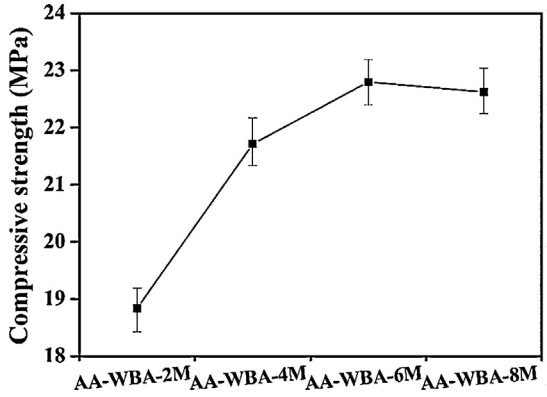

Fig. 9 – Compressive strength of AA-WBA samples.

the conversion coefficient compared to 40 mm cubic-shape standardised specimens is between 0.7 and 0.86. The compressive strength results obtained are low compared to a common OPC paste [58,59]. However, the results are substantially high compared to other studies which have been used WBA as sole precursor [33,35,37]. This fact is due to the use of 8–30 mm WBA fraction, which has a higher reactive SiO_2 availability than the whole WBA fraction [24]. In addition, the lower aluminium content in 8–30 mm fraction leads to a lower hydrogen generation [34]. It is also remarkable that SEM micrographs revealed a similar and high compactness in AA-WBA-4M, AA-WBA-6M, and AA-WBA-8M samples, in agreement with the compressive strength results.

Leaching test

From an environmental point of view, it was tried to simulate the worst possible scenario for the cements, which is the end of their lifecycle. This test was not intended to assess the potential release of the AA-WBA during their life service. The leaching test results were compared with the limits for acceptance in landfills for inert, non-hazardous, and hazardous waste according the criteria for the acceptance of waste established by the EU legislation [60]. The leaching concentration of heavy metal(loid)s in the leachates of WBA and AA-WBA are summarised in Table 5.

The WBA should be classified as non-hazardous waste because of the Sb value exceed the limit for acceptance in landfills as inert waste. In AA-WBA binders it is observed that heavy metal(loid)s are more leached than WBA due to the high pH of the alkali-activator solution. Most of the heavy metal(loid)s (Cr, Cu, Hg, Mo, Pb, and Zn) remained below the classification as non-hazardous waste and decreased their content as increase the NaOH concentration of the alkali-activator solution. However, As and Sb exceed the classification as non-hazardous waste. The presence of As and Sb is due to the large amount of container glass present in this WBA size fraction [32]. The glass industry uses As_2O_3 and Sb_2O_3 as a fining agent, to lighten glass, and to remove air bubbles [61]. It is important to note the aggressiveness of this test. It will be necessary in future investigations to carry out a more realistic test (monolithic test) considering that during the AA-WBA service life a gradual leaching will be produced due to the external agents (e.g. precipitations). The authors expected that better results would be obtained. However, it has been shown that the increase in Na_2O content in alkali-activator solution entails a negative effect to the leaching concentration of As and Sb.

Conclusions

The valorisation of WBA generated in the waste-to-energy facilities is an important challenge to the EU because of the large amount of this material produced yearly. The alkali activation of WBA is presented as an interesting alternative with a higher added value than its use as a secondary aggregate material. In addition, the use of WBA as a precursor would lead to a reduction in the consumption of the natural resources used to cement manufacturing. The present work revealed that least polluted fraction (from 8 to 30 mm) of WBA is a suitable precursor to formulate low-carbon cements at room temperature. No studies were found in the literature with such promising results of compressive strength using WBA as sole precursor. Although the composition of WBA showed a substantial lack of aluminium, the hydrolytic stability of the AA-WBA was verified. The selective chemical extractions and physicochemical characterisation indicated the formation of C–S–H, C–A–S–H, and/or (N,C)–A–S–H gels. XRD results were revealed the formation of secondary products as gaylussite. The effect of NaOH concentration in the AA-WBA was demonstrated since the higher the NaOH concentration, the higher formation of reaction products. The

Please cite this article in press as: A. Maldonado-Alameda, et al., Alkali-activated binders based on the coarse fraction of municipal solid waste incineration bottom ash, Bol. Soc. Esp. Cerám. Vidr. (2021), https://doi.org/10.1016/j.bsecv.2020.12.002

use of NaOH solution above 4 M led to the formation of a compact matrix which enhanced the mechanical behaviour. The compressive strength values reported herein also demonstrated that it is possible to develop alternative binders using WBA (from 8 to 30 mm fraction) as sole precursor. It was also proved that the better mechanical behaviour is obtained when the alkali-activator Ms is found between 2.0 and 2.5 range. Environmental characterisation showed that the increasing of NaOH concentration leads to a higher leaching concentration of As and Sb.

The authors consider that the main future line research should be the formulation of the AA-WBA mortars or concretes. The discarded fractions to formulate AA-WBA binders can be used as fine and coarse aggregates to enhance the AA-WBA binders' mechanical performance. In this way, the entire fractions of WBA would be valorised. Another research line could be based on the formulation of AA-WBA at different curing temperatures (e.g. 25–85 °C) to determine the effect of this parameter on the final properties of the binder. The increase of curing temperature must promote the formation of the main reaction products and improve the mechanical properties of the material. In addition, considering the lack of aluminium of these binders, the use of other raw materials aluminium-rich precursors could be used to favour the formation of reaction products, as well as to improve the mechanical properties and dilute the leaching concentration of heavy-metal(loid)s as the As and Sb.

Acknowledgements

The work is partially funded by the Spanish Government (BIA2017-83912-C2-1-R). The authors would like to thank the Catalan Government for the quality accreditation given to their research groups DIOPMA (2017 SGR 118), and to SIRUSA and VECSA for supplying the MSWI Bottom Ash. Mr Alex Maldonado-Alameda and Mr Jofre Mañosa are grateful to the Government of Catalonia for their research Grants (FI-DGR 2017 and FI-2020, respectively). Dr Jessica Giro-Paloma is a Serra Húnter Fellow.

REFERENCES

[1] D.N. Huntzinger, T.D. Eatmon, A life-cycle assessment of Portland cement manufacturing: comparing the traditional process with alternative technologies, J. Clean. Prod. 17 (2009) 668–675, http://dx.doi.org/10.1016/j.jclepro.2008.04.007.
[2] Mineral Commodity Summaries 2020, U.S. Geological Survey, Reston, VA, 2020, http://dx.doi.org/10.3133/mcs2020.
[3] A. Morandeau, M. Thiéry, P. Dangla, Impact of accelerated carbonation on OPC cement paste blended with fly ash, Cem. Concr. Res. 67 (2015) 226–236, http://dx.doi.org/10.1016/j.cemconres.2014.10.003.
[4] I.A. Chen, Synthesis of Portland Cement and Calcium Sulfoaluminate-Belite Cement for Sustainable Development and Performance, University of Texas at Austin, 2009, http://hdl.handle.net/2152/7537.
[5] E. Raffetti, M. Treccani, F. Donato, Cement plant emissions and health effects in the general population: a systematic review, Chemosphere 218 (2019) 211–222, http://dx.doi.org/10.1016/j.chemosphere.2018.11.088.
[6] C. Chen, G. Habert, Y. Bouzidi, A. Jullien, Environmental impact of cement production: detail of the different processes and cement plant variability evaluation, J. Clean. Prod. 18 (2010) 478–485, http://dx.doi.org/10.1016/j.jclepro.2009.12.014.
[7] G. Habert, C. Billard, P. Rossi, C. Chen, N. Roussel, Cement production technology improvement compared to factor 4 objectives, Cem. Concr. Res. 40 (2010) 820–826, http://dx.doi.org/10.1016/j.cemconres.2009.09.031.
[8] D.M. Roy, Alkali-activated cements: opportunities and challenges, Cem. Concr. Res. 29 (1999) 249–254, http://dx.doi.org/10.1016/S0008-8846(98)00093-3.
[9] C. Shi, A.F. Jiménez, A. Palomo, New cements for the 21st century: the pursuit of an alternative to Portland cement, Cem. Concr. Res. 41 (2011) 750–763, http://dx.doi.org/10.1016/j.cemconres.2011.03.016.
[10] C. Shi, P.V. Krivenko, D. Roy, Alkali-Activated Cements and Concretes, 1st ed., Taylor & Francis, London and New York, 2006.
[11] J.L. Provis, Alkali-activated materials, Cem. Concr. Res. 114 (2018) 40–48, http://dx.doi.org/10.1016/j.cemconres.2017.02.009.
[12] I. Garcia-Lodeiro, A. Palomo, A. Fernández-Jiménez, D.E. MacPhee, Compatibility studies between N–A–S–H and C–A–S–H gels. Study in the ternary diagram Na_2O–CaO–Al_2O_3–SiO_2–H_2O, Cem. Concr. Res. 41 (2011) 923–931, http://dx.doi.org/10.1016/j.cemconres.2011.05.006.
[13] A. Fernández-Jiménez, A. Palomo, Composition and microstructure of alkali activated fly ash binder: effect of the activator, Cem. Concr. Res. 35 (2005) 1984–1992, http://dx.doi.org/10.1016/j.cemconres.2005.03.003.
[14] T. Bakharev, J.G. Sanjayan, Y.B. Cheng, Effect of elevated temperature curing on properties of alkali-activated slag concrete, Cem. Concr. Res. 29 (1999) 1619–1625, http://dx.doi.org/10.1016/S0008-8846(99)00143-X.
[15] A.S. De Vargas, D.C.C. Dal Molin, A.C.F. Vilela, F.J. Da Silva, B. Pavão, H. Veit, The effects of Na_2O/SiO_2 molar ratio, curing temperature and age on compressive strength, morphology and microstructure of alkali-activated fly ash-based geopolymers, Cem. Concr. Compos. 33 (2011) 653–660, http://dx.doi.org/10.1016/j.cemconcomp.2011.03.006.
[16] F. Puertas, M. Palacios, H. Manzano, J.S. Dolado, A. Rico, J. Rodríguez, A model for the C–A–S–H gel formed in alkali-activated slag cements, J. Eur. Ceram. Soc. 31 (2011) 2043–2056, http://dx.doi.org/10.1016/j.jeurceramsoc.2011.04.036.
[17] O.G. Rivera, W.R. Long, C.A. Weiss, R.D. Moser, B.A. Williams, K. Torres-Cancel, E.R. Gore, P.G. Allison, Effect of elevated temperature on alkali-activated geopolymeric binders compared to portland cement-based binders, Cem. Concr. Res. 90 (2016) 43–51, http://dx.doi.org/10.1016/j.cemconres.2016.09.013.
[18] B.C. McLellan, R.P. Williams, J. Lay, A. Van Riessen, G.D. Corder, Costs and carbon emissions for geopolymer pastes in comparison to ordinary portland cement, J. Clean. Prod. 19 (2011) 1080–1090, http://dx.doi.org/10.1016/j.jclepro.2011.02.010.
[19] D. Xuan, P. Tang, C.S. Poon, MSWIBA-based cellular alkali-activated concrete incorporating waste glass powder, Cem. Concr. Compos. 95 (2019) 128–136, http://dx.doi.org/10.1016/j.cemconcomp.2018.10.018.
[20] T. Luukkonen, Z. Abdollahnejad, J. Yliniemi, P. Kinnunen, M. Illikainen, One-part alkali-activated materials: a review, Cem. Concr. Res. 103 (2018) 21–34, http://dx.doi.org/10.1016/j.cemconres.2017.10.001.
[21] Towards A Circular Economy: A Zero Waste Programme for Europe, Brussels, European Comission, 2014, https://eur-lex.

Please cite this article in press as: A. Maldonado-Alameda, et al., Alkali-activated binders based on the coarse fraction of municipal solid waste incineration bottom ash, Bol. Soc. Esp. Cerám. Vidr. (2021), https://doi.org/10.1016/j.bsecv.2020.12.002

europa.eu/resource.html?uri=cellar:aa88c66d-4553-11e4-a0cb-01aa75ed71a1.0022.03/DOC_1&format=PDF.
[22] A. Wongsa, K. Boonserm, C. Waisurasingha, V. Sata, P. Chindaprasirt, Use of municipal solid waste incinerator (MSWI) bottom ash in high calcium fly ash geopolymer matrix, J. Clean. Prod. 148 (2017) 49–59, http://dx.doi.org/10.1016/j.jclepro.2017.01.147.
[23] W. Zhu, X. Chen, L.J. Struble, E.H. Yang, Characterization of calcium-containing phases in alkali-activated municipal solid waste incineration bottom ash binder through chemical extraction and deconvoluted Fourier transform infrared spectra, J. Clean. Prod. 192 (2018) 782–789, http://dx.doi.org/10.1016/j.jclepro.2018.05.049.
[24] A. Maldonado-Alameda, J. Giro-Paloma, A. Svobodova-Sedlackova, J. Formosa, J.M. Chimenos, Municipal solid waste incineration bottom ash as alkali-activated cement precursor depending on particle size, J. Clean. Prod. 242 (2020) 1–10, http://dx.doi.org/10.1016/j.jclepro.2019.118443.
[25] CEWEP – Confederation of European Waste-to-energy, Latest Eurostat Figures: Municipal Waste Treatment 2018, 2020, https://www.cewep.eu/municipal-waste-treatment-2018/ (accessed 23.03.20).
[26] Eurostat – European Statistical Office, Municipal Waste by Waste Management Operations Statistics, 2020, https://appsso.eurostat.ec.europa.eu/nui/submitViewTableAction.do (accessed 23.03.20).
[27] CEWEP – Confederation of European Waste-to-energy, Bottom Ash Fact Sheet, 2019, pp. 1–2, https://www.cewep.eu/wp-content/uploads/2017/09/FINAL-Bottom-Ash-factsheet.pdf.
[28] D. Blasenbauer, F. Huber, J. Lederer, M.J. Quina, D. Blanc-Biscarat, A. Bogush, E. Bontempi, J. Blondeau, J.M. Chimenos, H. Dahlbo, J. Fagerqvist, J. Giro-Paloma, O. Hjelmar, J. Hyks, J. Keaney, M. Lupsea-Toader, C.J. O'Caollai, K. Orupõld, T. Pająk, F.-G. Simon, L. Svecova, M. Šyc, R. Ulvang, K. Vaajasaari, J. Van Caneghem, A. van Zomeren, S. Vasarevičius, K. Wégner, J. Fellner, Legal situation and current practice of waste incineration bottom ash utilisation in Europe, Waste Manag. 102 (2020) 868–883, http://dx.doi.org/10.1016/j.wasman.2019.11.031.
[29] R.V. Silva, J. de Brito, C.J. Lynn, R.K. Dhir, Use of municipal solid waste incineration bottom ashes in alkali-activated materials, ceramics and granular applications: a review, Waste Manag. 68 (2017) 207–220, http://dx.doi.org/10.1016/j.wasman.2017.06.043.
[30] J.M. Chimenos, A.I. Fernández, R. Nadal, F. Espiell, Short term natural weathering of MSWI bottom ash, J. Hazard. Mater. B 79 (2000) 287–299, http://dx.doi.org/10.1016/S0304-3894(00)00270-3.
[31] J.M. Chimenos, M. Segarra, M.A. Fernández, F. Espiell, Characterization of the bottom ash in municipal solid waste incinerator, J. Hazard. Mater. 64 (1999) 211–222, http://dx.doi.org/10.1016/S0304-3894(98)00246-5.
[32] R. del Valle-Zermeño, J. Gómez-Manrique, J. Giro-Paloma, J. Formosa, J.M. Chimenos, Material characterization of the MSWI bottom ash as a function of particle size. Effects of glass recycling over time, Sci. Total Environ. (2017) 581–582, http://dx.doi.org/10.1016/j.scitotenv.2017.01.047.
[33] Z. Chen, Y. Liu, W. Zhu, E.H. Yang, Incinerator bottom ash (IBA) aerated geopolymer, Constr. Build. Mater. 112 (2016) 1025–1031, http://dx.doi.org/10.1016/j.conbuildmat.2016.02.164.
[34] A. Saffarzadeh, N. Arumugam, T. Shimaoka, Aluminum and aluminum alloys in municipal solid waste incineration (MSWI) bottom ash: a potential source for the production of hydrogen gas, Int. J. Hydrogen Energy 41 (2015) 820–831, http://dx.doi.org/10.1016/j.ijhydene.2015.11.059.
[35] À. Maldonado-Alameda, J. Giro-Paloma, A. Alfocea-Roig, J. Formosa, J.M. Chimenos, Municipal solid waste incineration bottom ash as sole precursor in the alkali-activated binder formulation, Appl. Sci. 10 (2020) 1–15, http://dx.doi.org/10.3390/app10124129.
[36] Z. Tan, S.A. Bernal, J.L. Provis, Reproducible mini-slump test procedure for measuring the yield stress of cementitious pastes, Mater. Struct. Constr. 50 (2017) 1–12, http://dx.doi.org/10.1617/s11527-017-1103-x.
[37] W. Zhu, X. Chen, L.J. Struble, E. Yang, Characterization of calcium-containing phases in alkali-activated municipal solid waste incineration bottom ash binder through chemical extraction and deconvoluted Fourier transform infrared spectra, J. Clean. Prod. 192 (2018) 782–789, http://dx.doi.org/10.1016/j.jclepro.2018.05.049.
[38] S. Puligilla, P. Mondal, Co-existence of aluminosilicate and calcium silicate gel characterized through selective dissolution and FTIR spectral subtraction, Cem. Concr. Res. 70 (2015) 39–49, http://dx.doi.org/10.1016/j.cemconres.2015.01.006.
[39] W. Zhu, X. Chen, L.J. Struble, E.H. Yang, Quantitative characterization of aluminosilicate gels in alkali-activated incineration bottom ash through sequential chemical extractions and deconvoluted nuclear magnetic resonance spectra, Cem. Concr. Compos. 99 (2019) 175–180, http://dx.doi.org/10.1016/j.cemconcomp.2019.03.014.
[40] A. Fernández-Jiménez, A. Palomo, Mid-infrared spectroscopic studies of alkali-activated fly ash structure, Micropor. Mesopor. Mater. 86 (2005) 207–214, http://dx.doi.org/10.1016/j.micromeso.2005.05.057.
[41] Y. Ping, R.J. Kirkpatrick, P. Brent, P.F. McMillan, C. Xiandong, Structure of calcium silicate hydrate (C–S–H): near-, mid-, and far-infrared spectroscopy, J. Am. Ceram. Soc. 82 (1999) 742–748, http://dx.doi.org/10.1111/j.1151-2916.1999.tb01826.x.
[42] Z. Zhang, H. Wang, J.L. Provis, F. Bullen, A. Reid, Y. Zhu, Quantitative kinetic and structural analysis of geopolymers. Part 1. The activation of metakaolin with sodium hydroxide, Thermochim. Acta 539 (2012) 23–33, http://dx.doi.org/10.1016/j.tca.2012.03.021.
[43] I. García-Lodeiro, A. Fernández-Jiménez, M.T. Blanco, A. Palomo, FTIR study of the sol–gel synthesis of cementitious gels: C–S–H and N–A–S–H, J. Sol–Gel Sci. Technol. 45 (2008) 63–72, http://dx.doi.org/10.1007/s10971-007-1643-6.
[44] H.F.W. Taylor, Cement chemistry, Cem. Chem. (1997), http://dx.doi.org/10.1680/cc.25929.
[45] G. Huang, K. Yang, Y. Sun, Z. Lu, X. Zhang, L. Zuo, Y. Feng, R. Qian, Y. Qi, Y. Ji, Z. Xu, Influence of NaOH content on the alkali conversion mechanism in MSWI bottom ash alkali-activated mortars, Constr. Build. Mater. 248 (2020) 118582, http://dx.doi.org/10.1016/j.conbuildmat.2020.118582.
[46] G. Huang, Y. Ji, J. Li, L. Zhang, X. Liu, B. Liu, Effect of activated silica on polymerization mechanism and strength development of MSWI bottom ash alkali-activated mortars, Constr. Build. Mater. 201 (2019) 90–99, http://dx.doi.org/10.1016/j.conbuildmat.2018.12.125.
[47] M. Kovtun, E.P. Kearsley, J. Shekhovtsova, Chemical acceleration of a neutral granulated blast-furnace slag activated by sodium carbonate, Cem. Concr. Res. 72 (2015) 1–9, http://dx.doi.org/10.1016/j.cemconres.2015.02.014.
[48] B. Walkley, R. San Nicolas, M.A. Sani, G.J. Rees, J.V. Hanna, J.S.J. van Deventer, J.L. Provis, Phase evolution of C–(N)–A–S–H/N–A–S–H gel blends investigated via alkali-activation of synthetic calcium aluminosilicate precursors, Cem. Concr. Res. 89 (2016) 120–135, http://dx.doi.org/10.1016/j.cemconres.2016.08.010.
[49] A. Fernández-Jiménez, F. Puertas, I. Sobrados, J. Sanz, Structure of calcium silicate hydrates formed in

Please cite this article in press as: A. Maldonado-Alameda, et al., Alkali-activated binders based on the coarse fraction of municipal solid waste incineration bottom ash, Bol. Soc. Esp. Cerám. Vidr. (2021), https://doi.org/10.1016/j.bsecv.2020.12.002

alkaline-activated slag: influence of the type of alkaline activator, J. Am. Ceram. Soc. 86 (2003) 1389–1394, http://dx.doi.org/10.1111/j.1151-2916.2003.tb03481.x.
[50] M. Criado, A. Palomo, A. Fernández-Jiménez, Alkali activation of fly ashes. Part 1. Effect of curing conditions on the carbonation of the reaction products, Fuel 84 (2005) 2048–2054, http://dx.doi.org/10.1016/j.fuel.2005.03.030.
[51] F. Puertas, A. Fernández-Jiménez, M.T. Blanco-Varela, Pore solution in alkali-activated slag cement pastes. Relation to the composition and structure of calcium silicate hydrate, Cem. Concr. Res. 34 (2004) 139–148, http://dx.doi.org/10.1016/S0008-8846(03)00254-0.
[52] M. Criado, A. Fernández-Jiménez, A. Palomo, Alkali activation of fly ash: effect of the SiO_2O/Na_2OO ratio. Part I. FTIR study, Micropor. Mesopor. Mater. 106 (2007) 180–191, http://dx.doi.org/10.1016/j.micromeso.2007.02.055.
[53] W. Zhu, X. Chen, A. Zhao, L.J. Struble, E.H. Yang, Synthesis of high strength binders from alkali activation of glass materials from municipal solid waste incineration bottom ash, J. Clean. Prod. 212 (2019) 261–269, http://dx.doi.org/10.1016/j.jclepro.2018.11.295.
[54] A.M. Rashad, D.M. Sadek, H.A. Hassan, An investigation on blast-furnace stag as fine aggregate in alkali-activated slag mortars subjected to elevated temperatures, J. Clean. Prod. 112 (2016) 1086–1096, http://dx.doi.org/10.1016/j.jclepro.2015.07.127.
[55] S.D. Wang, K.L. Scrivener, P.L. Pratt, Factors affecting the strength of alkali-activated slag, Cem. Concr. Res. 24 (1994) 1033–1043, http://dx.doi.org/10.1016/0008-8846(94)90026-4.
[56] S. Choi, K.M. Lee, Influence of Na_2O content and Ms (SiO_2/Na_2O) of alkaline activator on workability and setting of alkali-activated slag paste, Materials (Basel) 12 (2019), http://dx.doi.org/10.3390/ma12132072.
[57] F.J. Alejandre, V. Flores-Alés, R. Villegas, J. García-Heras, E. Morón, Estimation of Portland cement mortar compressive strength using microcores. Influence of shape and size, Constr. Build. Mater. 55 (2014) 359–364, http://dx.doi.org/10.1016/j.conbuildmat.2014.01.049.
[58] Y.X. Li, Y.M. Chen, J.X. Wei, X.Y. He, H.T. Zhang, W.S. Zhang, A study on the relationship between porosity of the cement paste with mineral additives and compressive strength of mortar based on this paste, Cem. Concr. Res. 36 (2006) 1740–1743, http://dx.doi.org/10.1016/j.cemconres.2004.07.007.
[59] P. Chindaprasirt, C. Jaturapitakkul, T. Sinsiri, Effect of fly ash fineness on compressive strength and pore size of blended cement paste, Cem. Concr. Compos. 27 (2005) 425–428, http://dx.doi.org/10.1016/j.cemconcomp.2004.07.003.
[60] Council of the European Union, 2003/33/EC, Council Decision establishing criteria and procedures for the acceptance of waste at landfills pursuant to Article 16 of and Annex, II., to Directive 1999/31/EC, Off. J. Eur. Commun. (2003) 27–49.
[61] P. Apostoli, S. Giusti, D. Bartoli, A. Perico, P. Bavazzano, L. Alessio, Multiple exposure to arsenic, antimony, and other elements in art glass manufacturing, Am. J. Ind. Med. 34 (1998) 65–72, http://dx.doi.org/10.1002/(SICI)1097-0274(199807)34:1<65::AID-AJIM9>3.0.CO;2-P.

Please cite this article in press as: A. Maldonado-Alameda, et al., Alkali-activated binders based on the coarse fraction of municipal solid waste incineration bottom ash, Bol. Soc. Esp. Cerám. Vidr. (2021), https://doi.org/10.1016/j.bsecv.2020.12.002